



Copyright © 2003, Paper 7-010; 4,977 words, 9 Figures, 0 Animations, 1 Table.  
<http://EarthInteractions.org>

# Global Percent Tree Cover at a Spatial Resolution of 500 Meters: First Results of the MODIS Vegetation Continuous Fields Algorithm

**M. C. Hansen\***

Department of Geography, University of Maryland, College Park, Maryland

**R. S. DeFries**

Department of Geography, and Earth System Science Interdisciplinary Center, University of Maryland, College Park, Maryland

**J. R. G. Townshend**

Department of Geography, and Institute for Advanced Computer Studies, University of Maryland, College Park, Maryland

**M. Carroll, C. Dimiceli, and R. A. Sohlberg**

Department of Geography, University of Maryland, College Park, Maryland

Received 13 February 2003; accepted 5 May 2003

**ABSTRACT:** The first results of the Moderate Resolution Imaging Spectroradiometer (MODIS) vegetation continuous field algorithm's global percent tree cover are presented. Percent tree cover per 500-m MODIS pixel is

---

\* Corresponding author address: Dr. M. C. Hansen, Department of Geography, University of Maryland, College Park, College Park, MD 20742.

E-mail address: [mhansen@Glue.umd.edu](mailto:mhansen@Glue.umd.edu)

estimated using a supervised regression tree algorithm. Data derived from the MODIS visible bands contribute the most to discriminating tree cover. The results show that MODIS data yield greater spatial detail in the characterization of tree cover compared to past efforts using AVHRR data. This finer-scale depiction should allow for using successive tree cover maps in change detection studies at the global scale. Initial validation efforts show a reasonable relationship between the MODIS-estimated tree cover and tree cover from validation sites.

**KEYWORDS:** Global land cover, Forest mapping, Regression tree

## 1. Introduction

Standardized maps of global forest cover serve many purposes, among them the ability to estimate parameters for use in biogeochemical modeling procedures (Bonan et al., 2002; DeFries et al., 2002), in delineating remaining intact forest and woodland tracts for conservation and forestry concerns (Matthews, 2001), and in monitoring ecological succession and natural processes in forests. Such maps also reveal land use intensification when compared to potential vegetation conditions, revealing the human impact on naturally forested ecosystems. Repeated efforts over time can document change and aid in predicting future alterations to forest ecosystems. The synoptic view of global satellite datasets affords the best possibility of creating such maps. Initial efforts (DeFries et al. 1999; DeFries et al. 2000; Zhu and Waller 2001; Hansen et al. 2002) have demonstrated this capability.

This paper describes the creation of a new global percent tree cover map based on 500-m data from the Moderate Resolution Imaging Spectroradiometer (MODIS) instrument on board the National Aeronautics and Space Administration's (NASA's) *Terra* spacecraft and represents the finest-scale global forest information to date. The MODIS sensor represents a significant gain in spatial detail due primarily to three facts. The first is the finer instantaneous field of view of MODIS (250 and 500 m<sup>2</sup>) as compared to heritage Advanced Very High Resolution Radiometer (AVHRR) instruments (1 km<sup>2</sup>). Second, due to the fact that MODIS was built with seven bands specifically designed for land cover monitoring, there is an improved spectral/spatial response compared to AVHRR. This allows for greater accuracy in mapping due to more robust spectral signatures. It also aids in reducing background scattering from adjacent pixels, as the MODIS land bands were designed to limit the impact of atmospheric scattering. Third, 500-m red and near-infrared data, two bands important for land cover mapping, are created from averaged 250-m imagery. This resampling also reduces the percent contribution of adjacency effects on 500-m pixels for these bands, allowing for improved land cover estimates (Townshend et al., 2000). The result is a dataset that reveals far more spatial detail than previous efforts. Maps such as the MODIS global continuous field of percent tree cover map should be of use to more varied scientific applications than previous coarse-scale maps.

Proportional per pixel tree cover estimates, or continuous fields of percent tree cover, are an improved thematic representation over discrete classifications (DeFries et al., 1995). Continuous field maps yield improved depictions of spatially

complex landscapes and the ability to use successive depictions to measure change (Hansen and DeFries, 2003). Numerous methodologies exist to portray subpixel vegetative cover. The techniques including fuzzy estimations of forest cover (Foody and Cox, 1994), plant density isolines within multispectral scatterplots (Jasinski, 1996; Zhu and Waller, 2001), empirically calibrated estimates using multiresolution datasets (Zhu and Evans, 1994; Iverson, 1989; DeFries et al., 1997), other multiresolution estimates that incorporate spatial arrangement (Mayaux and Lambin, 1997), and endmember linear mixture modeling (DeFries et al., 2000; Adams et al., 1995; Settle and Drake, 1993). This paper builds on prior studies using AVHRR data to derive a global MODIS 500-m percent tree cover map. The approach is an empirical, multiresolution calibration method that uses a regression tree algorithm to estimate the percent tree canopy cover (Hansen et al., 2002). The regression tree is a nonlinear, flexible model appropriate for handling the variability present in global vegetation phenology. It also allows for the calibration of the model along the entire continuum of tree cover, avoiding the problems of using only endmembers for calibration.

## 2. Data

This initial attempt using MODIS imagery employed approximately 1 year of data. The inputs consisted of 8-day minimum blue reflectance composites that were made in order to reduce the presence of clouds in the datastream. However, this procedure can lead to the inclusion of pixels within areas of cloud shadow. To reduce the presence of cloud shadows, the data were converted to 40-day composites using a second darkest albedo (sum of blue, green, and red bands) algorithm. The inputs date from 31 October 2000 to 9 December 2001. An extra 40-day composite period was added to attempt to compensate for data gaps resulting from temporary sensor outages.

The seven MODIS land bands were used as inputs: blue (459–479 nm), green (545–565 nm), red (620–670 nm), near infrared (841–876 nm), and midinfrared (1230–1250, 1628–1652, 2105–2155 nm). The MODIS-composited data were transformed into annual metrics that capture the salient points in the phenologic cycle. A total of 68 metrics were derived from the composited data for bands 1–7 and the Normalized Difference Vegetation Index (NDVI). These were used as the inputs for estimating percent tree cover. Metrics such as maximum annual NDVI or mean growing season red reflectance represent generic signatures that can be used to map global vegetation. The approach to deriving the metrics and training data is fully described in Hansen et al. (Hansen et al., 2002).

Only the red and near-infrared MODIS bands are close to the bandwidths in the long-term AVHRR sensor's record. In addition to these two bands, AVHRR has one midinfrared and two thermal bands that record brightness temperatures and proved invaluable to mapping global land cover (Hansen et al., 2000). The temperature bands act as surrogates for biome-level climatic variability. For example, tropical drought deciduous woodlands can be stratified from tropical humid forests using thermal brightness metrics. There is less evapotranspiration during dry periods in seasonal woodlands, and this causes an increase in surface temperature that is captured in the thermal bands.

While the MODIS sensor has bands for measuring surface temperature [band 31 (10780–11280 nm) and band 32 (11770–12270 nm)], they are not currently processed for use in land cover mapping. There is a surface temperature product (Wan et al., 2002) that employs these bands, but its algorithms are land cover dependent, precluding its use in mapping surface cover. Bands 31 and 32 of the MODIS instrument are used to derive surface temperature. They mimic the AVHRR thermal bands, and their inclusion in future reprocessing of the land products is recommended. In place of the missing MODIS thermal data, which act as a key regional stratification signal (Hansen et al., 2002), other features were included. First, a three-region layer was included as a metric: extratropical north (approximately 23°N and above), tropical (approximately between plus and minus 23° latitude), and extratropical south (approximately 23°S and below). Second, an archival 1-km AVHRR channel-4 brightness temperature (10300–11300 nm) signal was used in metric form. These data are from 1995 to 1996 and represent the most recent globally processed thermal images at 1 km for the AVHRR. The thermal information is used within the algorithm to regionally stratify the globe, as previously stated, and should not be significantly affected by land cover change events since the time of the data's acquisition. The thermal data exist at a 1-km spatial resolution, and any land cover change in the interim would have to be very extensive to impact the thermal signal. Even in these instances, the MODIS data at a finer scale correspond to the detail in the training data, and these data should drive most of the characterization. The AVHRR metrics and regional layers are used alongside the MODIS data inputs.

The training data are derived by aggregating over 250 classified high-resolution Landsat images to the MODIS grid. The Landsat images were classified into four classes of tree cover, each class having a mean percent tree cover label. By averaging the Landsat tree cover strata to MODIS cells, a 500-m continuous training dataset was created. This training dataset contains over a million pixels, which were systematically sampled to create a final training dataset of 271,149 pixels at the 500-m MODIS resolution. These training data have been used in a number of global land cover mapping exercises and descriptions of their derivation and distribution can be found in previous refereed studies (DeFries et al., 1998; Hansen et al., 2000; Hansen et al., 2002).

### **3. Methods**

The MODIS continuous fields of vegetation cover algorithm is described in Hansen et al. (Hansen et al., 2002). It is an automated procedure that employs a regression tree algorithm (Venables and Ripley, 1994). The regression tree is a nonlinear, distribution-free algorithm that is highly suited for handling the complexity of global spectral land cover signatures. The training data are used as the dependent variable, predicted by the independent variables in the form of the annual MODIS metrics. Outputs from the regression tree are further modified by a stepwise regression and bias adjustment per Hansen et al. (Hansen et al., 2002). The derivation of tree cover in this way creates the possibility of using subsequent depictions to measure change. Hansen and DeFries (Hansen and DeFries, 2003)

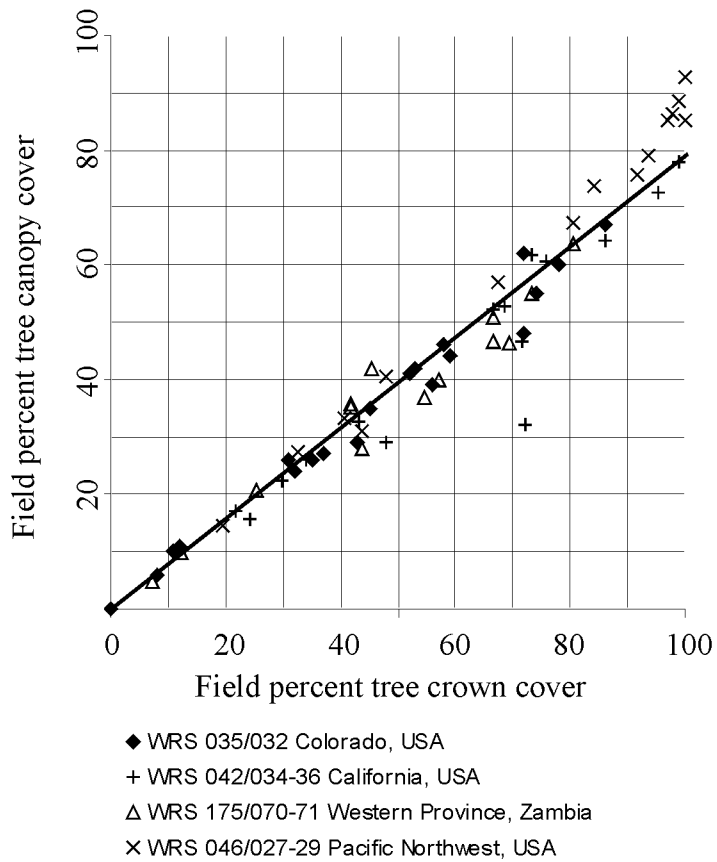


Figure 1. Plot of validation field data from four test areas, each covering a wide range of tree cover density, where  $y = 0.79x$  and  $R^2 = 0.95$ . See Hansen et al. (Hansen et al., 2002a) for example from Zambia test area.

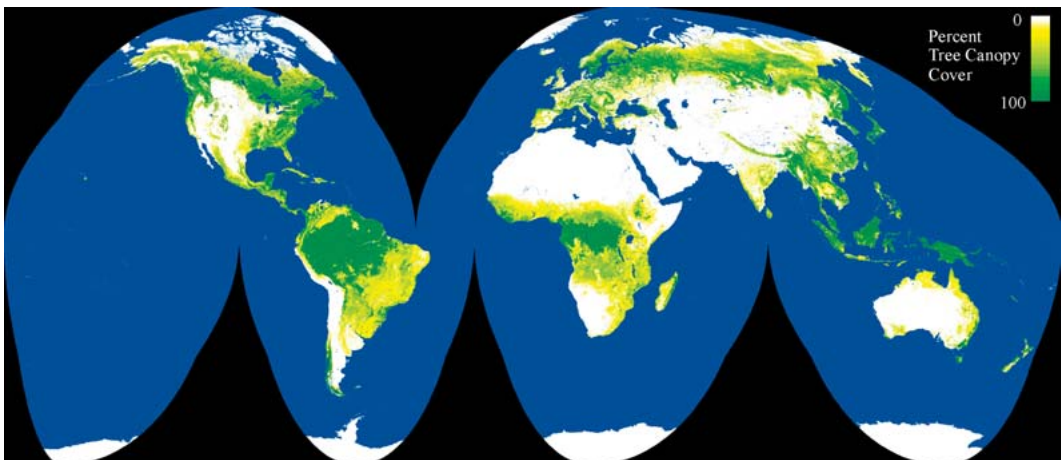


Figure 2. Final percent tree cover map in the Interrupted Goode Homolosine projection.

**Table 1. Percent contribution to the overall reduction of sum of squares in the regression tree structure aggregated in the following ways: (a) regression tree splits aggregated by the band used in the metrics with total number of splits in parentheses, (b) splits aggregated by individual metric with total number of splits in parentheses and only the best 10 metrics shown, (c) metrics used in the 10 best individual splits in reducing overall sum of squares. These splits are highlighted in the tree structure of Figure 4. For mean metrics the span of time is listed by number of 40-day composites. For MODIS bands 1–7, metrics are derived by looking at dark albedo values. For example, mean 1–3 band 6 represents the mean of the three darkest band 6 composite values. NDVI and temperature means are based on finding the maximum ranked composites. For example, mean 1–5 NDVI is the five highest NDVI composites averaged. The only exceptions to this are the metrics binned using NDVI as a reference. For example, in mean 1–3g band 1, the “g” indicates that the band 1 values are found which correspond to the three greenest composites based on ranked NDVI values. Thus, mean 1–3g band 1 is a mean red reflectance value, which corresponds to the three greenest composites.**

Percent reduction in overall sum of squares per metrics aggregated by band	Percent reduction in overall sum of squares per individual metric	Percent reduction in overall sum of squares per regression tree split			
Band 1 metrics (9)	68.1	Mean 1–3g band 1 (4)	67.7	Mean 1–3g band 1	60.1
Band 3 metrics (21)	9.6	Mean 1–3g band 3 (2)	6.7	Mean 1–3g band 1	7.3
Band 4 metrics (20)	5.4	Mean 1–3 temperature (6)	4.4	Mean 1–3g band 3	6.7
Temperature metrics (13)	5.1	Mean 1–3 band 6 (3)	3.6	Mean 1–3 band 6	3.3
NDVI metrics (14)	4.5	Rank 3 band 3 (16)	2.7	Mean 1–3 temperature	2.4
Band 6 metrics (5)	3.8	Mean 1–3 band 4 (5)	2.7	Mean 1–3 temperature	1.8
Band 5 metrics (10)	1.3	Mean 1–8 NDVI (3)	2.2	Mean 1–3 band 4	1.4
Regions (7)	1.0	Mean 1–8 band 4 (5)	1.6	Mean 1–8 NDVI	1.2
Band 2 metrics (5)	1.0	Mean 1–5 NDVI (6)	1.3	Mean 1–5 NDVI	1.1
Band 7 metrics (4)	0.2	Regions (7)	1.0	Mean 1–8 NDVI	0.9

used such an approach in detecting change based on the long-term AVHRR 8-km Pathfinder dataset.

The output of the algorithm is the percent canopy cover per 500-m MODIS pixel. Here percent canopy refers to the amount of skylight obstructed by tree canopies equal to or greater than 5 m in height and is different than percent crown cover (crown cover = canopy cover + within crown skylight). The canopy cover definition is used in vegetation modeling exercises in which light availability is an important parameter. Foresters, on the other hand, largely employ crown cover in measuring forest density. Crown cover is a better measure when performing areal inventories and is the variable used in many forest accounting procedures.

To better understand this relationship, ongoing field work is being performed where both crown and canopy cover values are measured. Initial work suggests that the mean forest label used in deriving canopy cover (80%) training data corresponds to a 100% forested area in terms of crown cover. Figure 1 shows field data gathered from four different sites to test this assumption and shows a

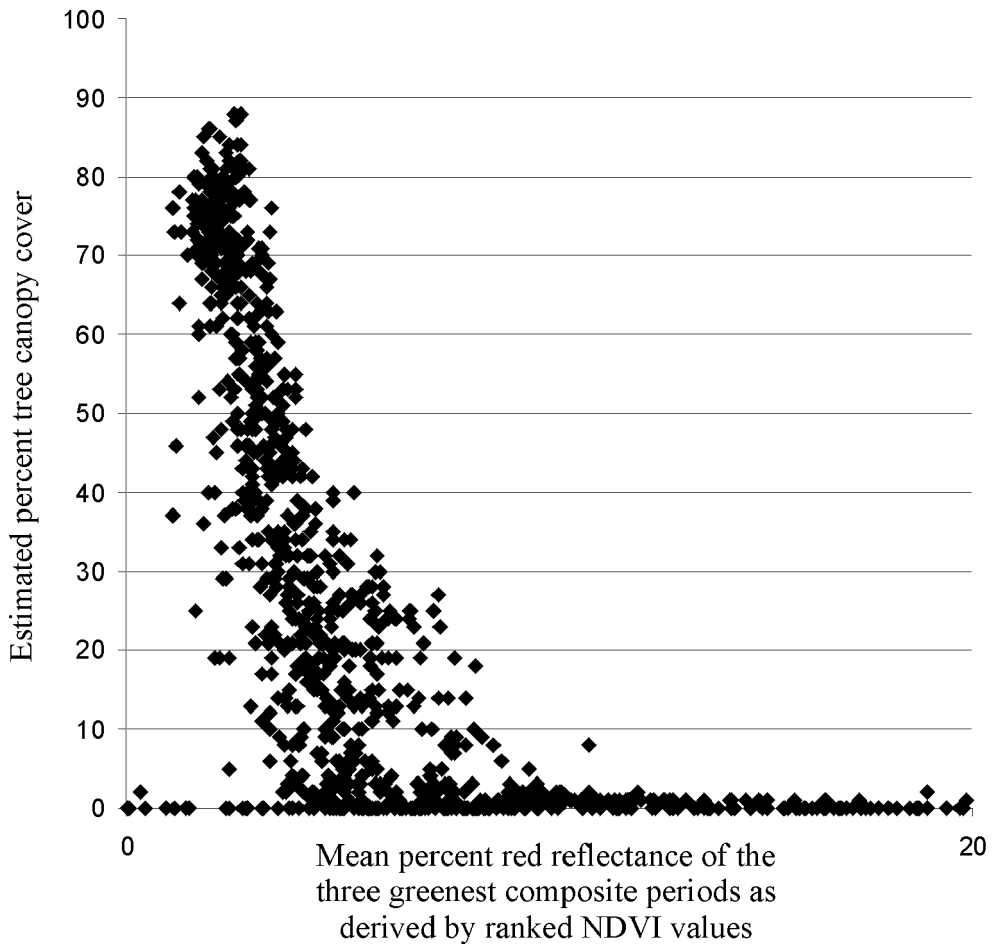


**Figure 3. Plot of band-1 metric (mean red reflectance of the three greenest compositing periods) vs estimated tree cover for a sample of 1000 pixels.**

reasonable relationship. Of course, different tree types have different relationships between canopy and crown cover. Fir trees, for example, generally have little light availability within the canopy. Four subalpine fir sites from Colorado reveal a 0.9 ratio of canopy to crown cover. Broadleaf Kalahari woodland trees in western Zambia, on the other hand, have a greater presence within crown gaps and a 0.76 ratio. Information on stand species is not available at the global scale; however, the 0.8 slope in Figure 1 suggests a reasonable estimate for converting between canopy and crown cover. It is suggested that users interested in deriving the crown cover variable should divide the canopy cover layer by 0.8.

#### 4. Results

The resulting regression tree yielded 109 terminal nodes. The largest node in terms of surface area maps most of the tropical broadleaf evergreen forest and accounts

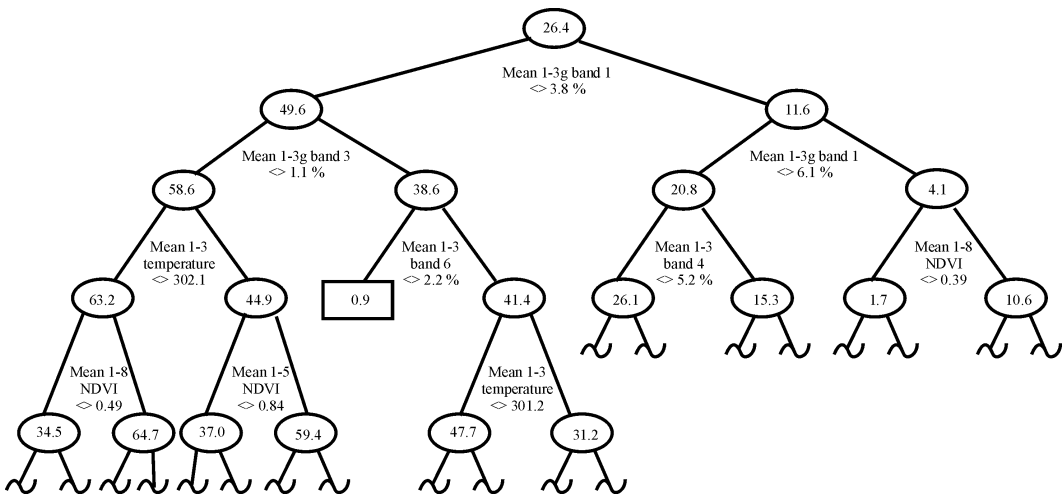


**Figure 4. Regression tree object before stepwise regression and bias adjustment steps. Estimated percent tree cover at the intermediate nodes is shown within the ellipses. The metric used at each split is shown below each of these nodes. Only one terminal node is shown as a rectangle; the tilde (~) indicates more splits in the lower portion of the regression tree.**

for over 20% of dense (>40%) tree cover globally. This is a fairly homogeneous cover type with a characteristic signature. The regression tree delineated two subclasses of this forest type that represent more confused spectral signatures: persistently cloudy areas and areas of regrowth/disturbance. The next largest node in terms of tree cover maps dense needleleaf boreal forest. The final map is shown in Figure 2.

The regression tree object can be studied to reveal which spectral information drives the tree cover characterization. Table 1 shows which metrics add the most to reducing the overall sum of squares in delineating tree cover strata. From Table 1, note that the mean red reflectance corresponding to the three greenest composite periods' metric contributes most to mapping tree cover. Of the overall reduction in the sum of squares, this metric alone contributes nearly 70% of the reduction. The first split in the regression tree uses this metric, and this single split accounts for 60% of the reduction in the sum of squares. This metric is plotted against the resulting estimated tree cover for a 1000-pixel sample in Figure 3. While this metric alone cannot map global tree cover, it is clear that increasing canopy density is correlated with lower red reflectance values due to the combined effects of canopy shadowing and chlorophyll absorption.

Of interest is the fact that the MODIS visible bands (red, green, and blue) all contribute significantly, while the near- and midinfrared bands largely do not. Only band 6 performs comparably with the visible bands and is critical to mapping inundated grasslands. This is a midinfrared band with strong water absorption qualities that capture seasonal flooding events. Figure 4 shows the top levels of the regression tree and how band 6 is used to map these grasslands. Although the

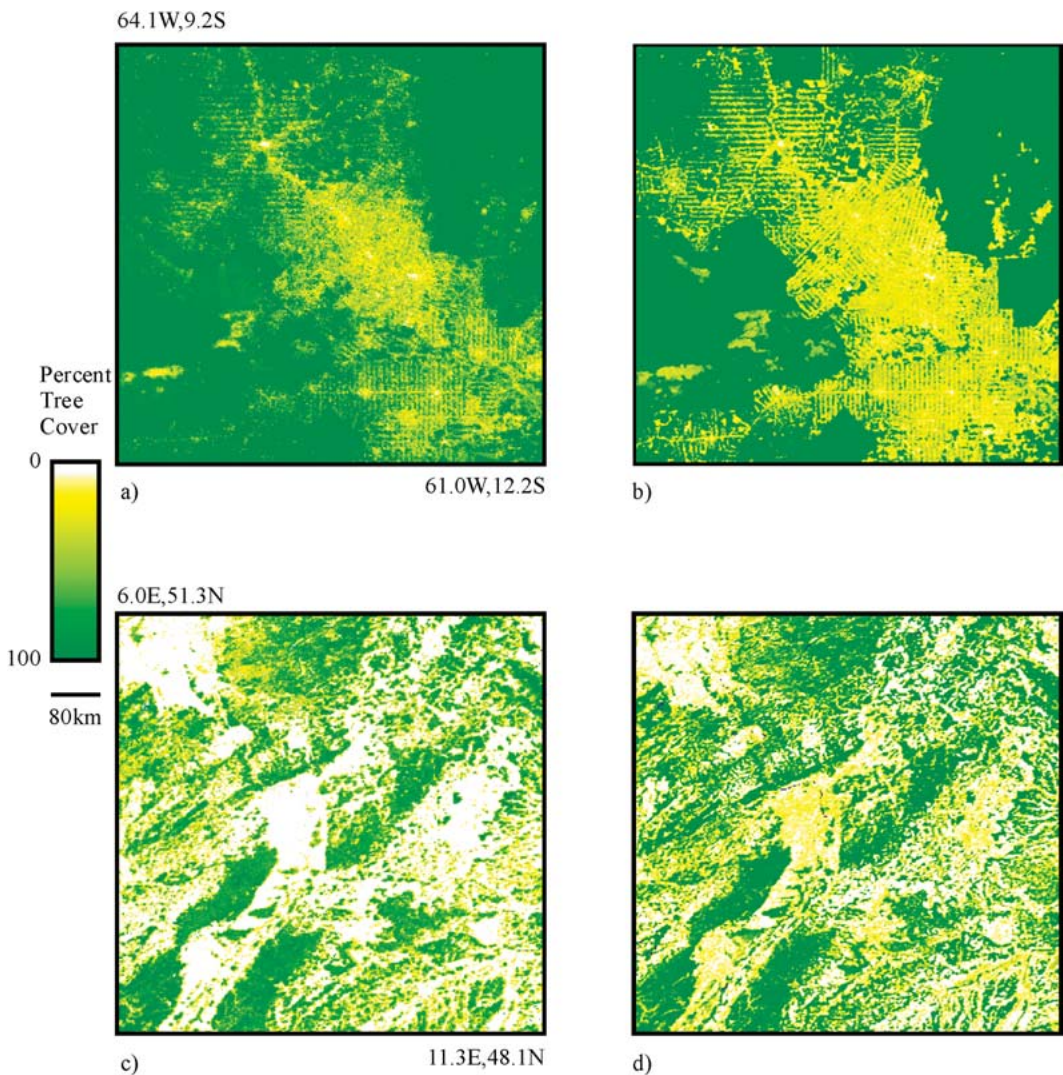


**Figure 5.** Two subsets comparing the 2000–01 500-m MODIS tree cover map with a 1995–96 1-km AVHRR tree cover map. (a) Area of Rondônia, Brazil, from the AVHRR map, (b) same area from the 2000–01 MODIS map, (c) area along the French–German border from the AVHRR map, and (d) same area from the MODIS map.

infrared bands do not feature prominently, NDVI, derived using the near infrared, is useful as seen in Table 1. It should also be noted that many of the most used metrics of the visible bands are binned using NDVI to identify the greenest times of the year.

The thermal signal of the AVHRR was used repeatedly, as seen in Table 1, and underscores the need to include the MODIS thermal signal in the gridded land products. The regional stratification was not as useful, only accounting for 1% of

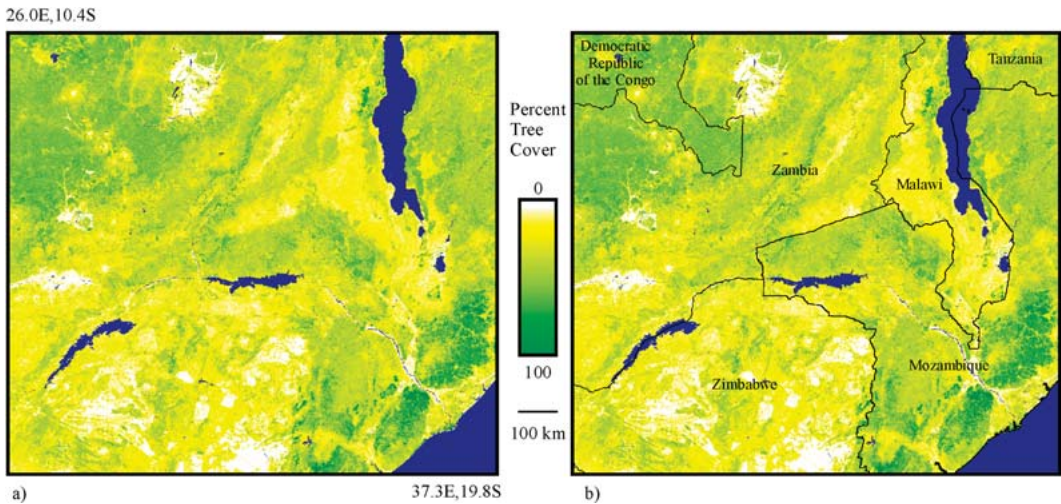


**Figure 6.** Transnational boundary differences in percent tree cover. The highest population density in this subset is found in Malawi, which is shown to have greater clearing of tree cover than adjacent countries. Mozambique is less disturbed as evidenced by the Tete Province jutting into the more intensively used landscapes of Zimbabwe, Zambia, and Malawi. The arm of the Congo extending into Zambia's copper belt is less disturbed than the heavily developed lands across the border.

the overall reduction in the sum of squares. Two kinds of metrics were of little use: amplitude metrics for measuring the absolute spectral change of cover through the growing season and metrics associated with single-peak greenness dates, which were largely unused by the regression tree.

The map has greatly increased spatial detail as compared to the AVHRR-derived maps. Figure 5 shows two areas as examples. The human imprint on the landscape is more readily seen as compared to the AVHRR example. There is the reasonable expectation that consecutive comparisons of annual maps should reveal change. Discrete breaks in tree cover due to administrative status, such as a national park, government-owned lands, and transnational variations in land use intensity, are clearly evident throughout the map. Figure 6 shows a region of southeastern Africa where differential land use intensification is visible across national boundaries. The rich detail present should be of use to land managers working at a regional scale and in need of an internally consistent map. Fire history is present as well, particularly in the boreal zone, as shown in Figure 7 by the number of quasi-elliptical patterns that correspond to known fire scars. Further analysis of these data should reveal if this kind of map can be used to determine likely succession patterns, especially when other vegetation continuous field layers, such as leaf type, are generated.

The map will be updated annually and used to monitor change in global tree cover. Figure 8 shows the MODIS percent tree cover map with an overlay of a change study using AVHRR data for 1982–99 (Hansen and DeFries, 2003).

154.5W,68.8N

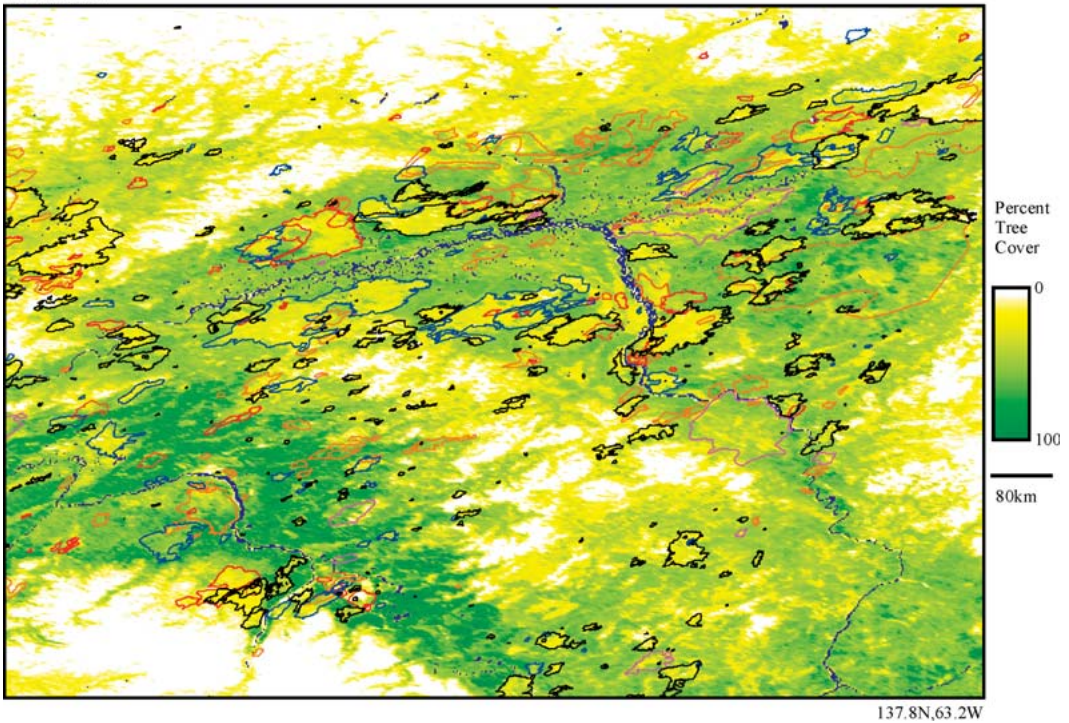


**Figure 7.** MODIS data with burn scar overlay. Black vectors represent burn scars from 1990–2000, blue 1980–89, red 1970–79, magenta 1960–69, and orange 1950–59. More recent scars are fairly well delineated in the tree cover percentage map. Data are from Murphy et al. (Murphy et al., 2000) and consist of a combination of ground and aerial surveys and satellite image interpretations.

MODIS data from the 250- and 500-m bands should capture change in forest cover more accurately. Optimum change study intervals, whether annual or 5–10-yr epochs, will be sought. Improvements to the methodology, such as the inclusion of MODIS thermal bands, will be implemented as soon as is feasible.

## 5. Validation

A multiresolution mapping approach in conjunction with field data is being used at a number of sites to develop validation data for the percent tree cover map. The exercise includes using field data along with *IKONOS* and Enhanced Thematic Mapper Plus (ETM+) data to create validation test areas the size of an ETM+ image. Crown cover maps of *IKONOS* images are binned to ETM+ cells and used as continuous training data to map the percent crown cover for 30-m pixels. This ETM+ crown cover map is then averaged to a 500-m resolution to validate the MODIS map. Performing this exercise in a wide variety of biomes will help to create a test bed against which successive iterations of the tree cover product can be

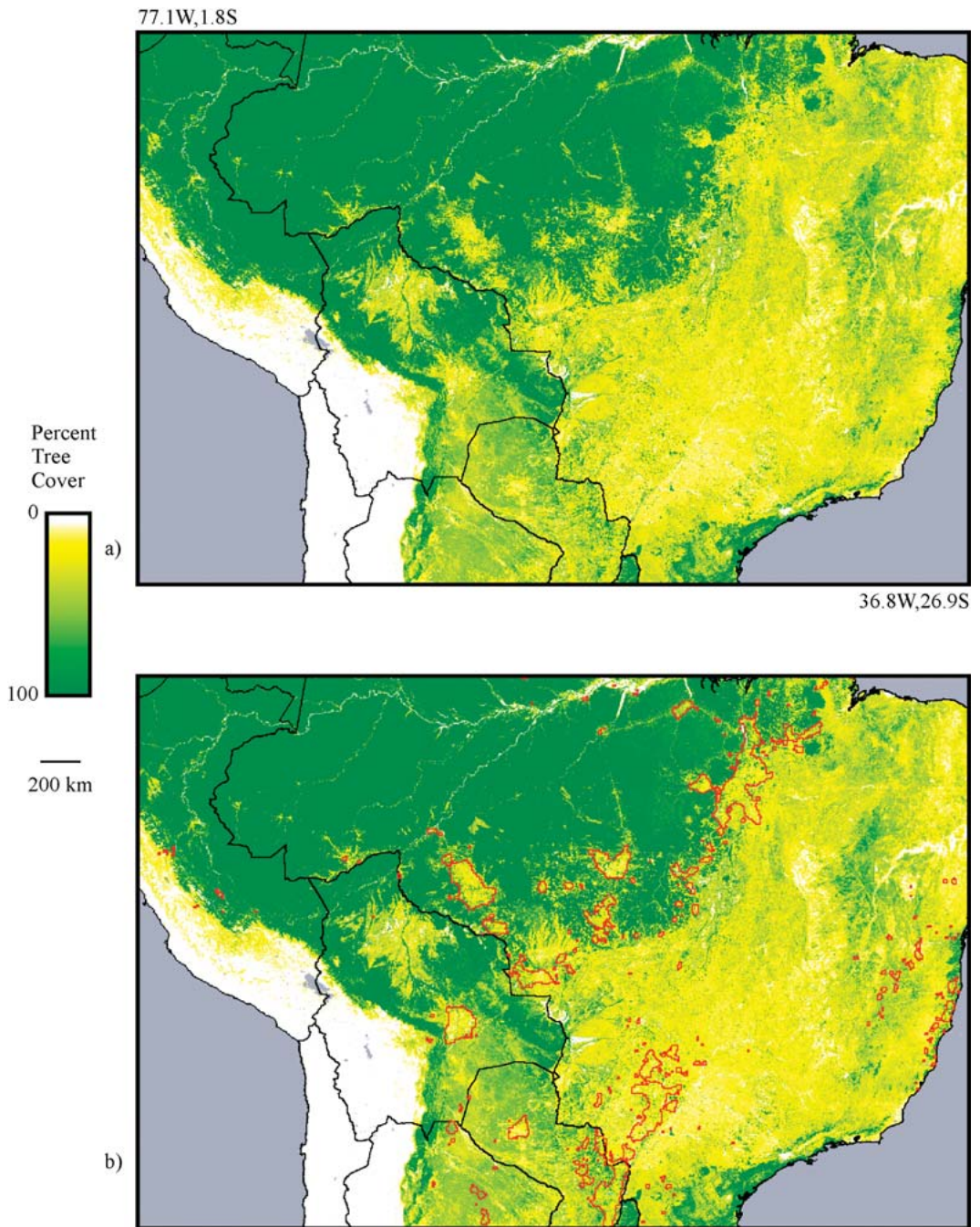
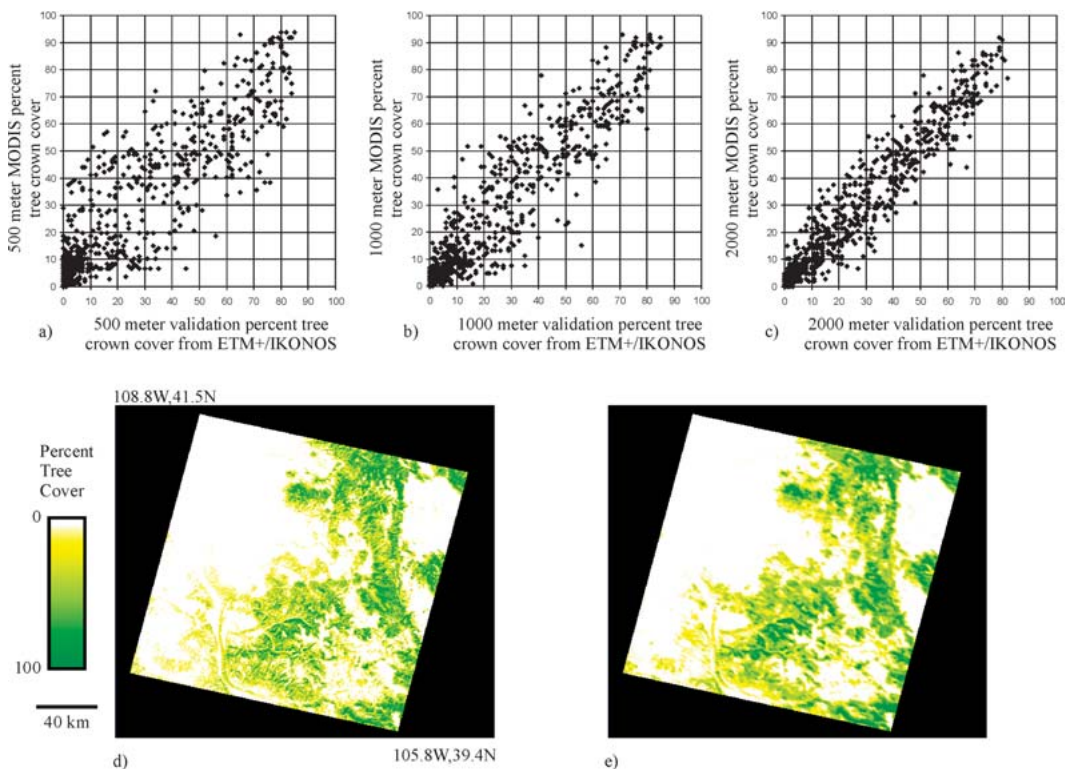


Figure 8. A portion of South American tree cover with deforestation hot spot overlay. The change areas are from a 19-yr study of 8-km AVHRR data (Hansen and Defries, 2003).



**Figure 9.** Validation data from CO WRS 035/032. (a) Plot of 500-m MODIS-estimated percent tree crown cover vs 500-m crown cover validation data derived from *IKONOS/Enhanced Thematic Mapper Plus/field* data study,  $y=0.99$ ,  $R^2=0.81$ . (b) Data averaged to a 1-km resolution,  $y=1.05x$ ,  $R^2=0.89$ . (c) Data averaged to a 2-km spatial resolution,  $y=1.06x$ ,  $R^2=0.94$ . (d) Validation data percent tree crown cover. (e) MODIS-estimated percent tree crown cover at 500-m resolution.

validated. The method has been initially tested for a Western Province, Zambia, woodland site (Hansen et al., 2002) and is now being used in other areas.

Figure 9 shows results from a Colorado test area. Averaging the product dramatically improves the validation measures. The greater scatter at 500-m spatial resolution is probably an artifact of resampling in the MODIS data. As with all global data processing, a nearest-neighbor scheme is used to reduce processing time. This approach leads to a geometric degradation of the signal as the process is repeated throughout the compositing process. Averaging the product to a 1-km spatial resolution appears to ameliorate some of these effects.

## 6. Conclusions

The first layer of the MODIS Vegetation Continuous Field product, percent tree canopy cover, has been generated and is available for use ( The MODIS product in tile format for canopy cover is available online at the EROS data center <http://>

edcimswww.cr.usgs.gov/pub/imswelcome and per continent at glcf.umiacs.umd.edu). The map reveals the improved spatial/spectral characteristics in the MODIS data compared to heritage AVHRR data. This should lead to a wider variety of applications that employ the MODIS-derived maps. Visible bands in the MODIS data provided the most discrimination along with NDVI and AVHRR brightness temperatures. This points out the need to add thermal information to the MODIS land datastream. Currently in production are other vegetation layers, including the percentages of herbaceous/shrub, bare ground, tree leaf type, and leaf longevity. Upon completion, these maps should enhance the current understanding of global land cover distributions and provide a basis for monitoring land cover change globally.

## References

- Adams, J. B., D. E. Sabol, V. Kapos, R. A. Filho, D. A. Roberts, M. O. Smith, and A. R. Gillespie, 1995: Classification of multispectral images based on fraction endmembers: Application to land-cover change in the Brazilian Amazon. *Remote Sens. Environ.*, **52**, 137–154.
- Bonan, G. B., S. Levis, L. Kergoat, and K. W. Oleson, 2002: Landscapes as patches of plant functional types: An integrating concept for climate and ecosystem models. *Global Biogeochem. Cycles*, **16**, 1360–1384.
- DeFries, R. S., et al., 1995: Mapping the land surface for global atmosphere–biosphere models: Towards continuous distributions of vegetation’s functional properties. *J. Geophys. Res.*, **100**, 20,867–20,882.
- DeFries, R. S., M. C. Hansen, J. R. G. Townshend, and R. S. Sohlberg, 1998: Global land cover classifications at 8km spatial resolution: The use of training data derived from Landsat imagery in decision tree classifiers. *Int. J. Remote Sens.*, **19**, 3141–3168.
- DeFries, R. S., J. R. G. Townshend, and M. C. Hansen, 1999: Continuous fields of vegetation characteristics at the global scale at 1-km resolution. *J. Geophys. Res.*, **104**, 16,911–16,923.
- DeFries, R. S., M. C. Hansen, J. R. G. Townshend, and A. C. Janetos, 2000: A new global 1-km dataset for percentage tree cover derived from remote sensing. *Global Change Biol.*, **6**, 247–254.
- DeFries, R. S., R. A. Houghton, M. C. Hansen, C. B. Field, D. Skole, and J. Townshend, 2002: Carbon emissions from tropical deforestation and regrowth based on satellite observations for the 1980’s and 1990’s. *Proc. Natl. Acad. Sci.*, **99**, 14,256–14,261.
- Foody, G., and D. Cox, 1994: Sub-pixel land cover composition estimation using a linear mixture model and fuzzy membership functions. *Int. J. Remote Sens.*, **15**, 619–631.
- Hansen, M. C., and R. S. DeFries, 2003: Detecting long term global forest change using continuous fields of tree cover maps from 8km AVHRR data for the years 1982–1999. *Ecosystems*, in press.
- Hansen, M. C., R. S. DeFries, J. R. G. Townshend, and R. Sohlberg, 2000: Global land cover classification at 1km spatial resolution using a classification tree approach. *Int. J. Remote Sens.*, **21**, 1331–1364.
- Hansen, M. C., R. S. DeFries, J. R. G. Townshend, L. Marufu, and R. Sohlberg, 2002a: Development of a MODIS tree cover validation data set for Western Province, Zambia. *Remote Sens. Environ.*, **83**, 320–335.
- Hansen, M. C., R. S. DeFries, J. R. G. Townshend, R. A. Sohlberg, C. Dimiceli, and M.

- Carroll, 2002b: Towards an operational MODIS continuous field of percent tree cover algorithm: Examples using AVHRR and MODIS data. *Remote Sens. Environ.*, **83**, 303–319.
- Jasinski, M. F., 1996: Estimation of subpixel vegetation density of natural regions using satellite multispectral imagery. *IEEE Trans. Geosci. Remote Sens.*, **34**, 804–813.
- Matthews, E., 2001: Understanding the FRA. World Resources Institute Forest Briefing *No. 1*, World Resources Institute, Washington, D.C., XX pp.
- Mayaux, P., and E. F. Lambin, 1997: Tropical forest area measured from global land cover classifications: Inverse calibration models based on spatial textures. *Remote Sens. Environ.*, **59**, 29–43.
- Murphy, P. J., J. P. Mudd, B. J. Stocks, E. S. Kasischke, D. Barry, M. E. Alexander, and N. H. F. French, 2000: Historical fire records in the North American boreal forest, in *Fire Climate Change, and Carbon Cycling in the Boreal Forest*, edited by E. Kasischke and B. Stocks, Springer-Verlag, New York, 274–288.
- Settle, J., and N. A. Drake, 1993: Linear mixing and the estimation of ground cover proportions. *Int. J. Remote Sens.*, **14**, 1159–1177.
- Townshend, J. R. G., C. Huang, S. N. V. Kalluri, R. S. Defries, S. Liang, and K. Yang, 2000: Beware of per-pixel characterization of land cover. *Int. J. Remote Sens.*, **21**, 839–843.
- Venables, W. N., and B. D. Ripley, 1994: *Modern Applied Statistics with S-Plus*. Springer-Verlag, New York, 462 pp.
- Wan, Z., Y. Zhang, Q. Zhang, and Z. Li, 2002: Validation of the land-surface temperature products retrieved from Terra Moderate Resolution Imaging Spectroradiometer data. *Remote Sens. Environ.*, **83**, 163–180.
- Zhu, Z., and D. L. Evans, 1994: U.S. forest types and predicted percent forest cover from AVHRR data. *Photogramm. Eng. Remote Sens.*, **60**, 525–531.
- Zhu, Z., and E. Waller, 2001: Global forest cover mapping for the United Nations Food and Agriculture Organization Forest Resources Assessment 2000 Program. UNFAO, Rome, Italy, XX pp.